

Article

Experimental Study on the Effect of Soil Reinforcement and Slip Resistance on Shallow Slopes by Herbaceous Plant Root System

Jinguo Lv^{1,2,*}, Wenqi Wang¹, Te Dai³, Baoyong Liu³ and Guangwei Liu¹

¹ College of Mining, Liaoning Technical University, Fuxin 123000, China; 13137881013@163.com (W.W.); liuguangwei@lntu.edu.cn (G.L.)

² School of Mechanics and Engineering, Liaoning Technical University, Fuxin 123000, China

³ College of Environmental Science and Engineering, Liaoning Technical University, Fuxin 123000, China; daitu2008@163.com (T.D.); liubaoyong00@163.com (B.L.)

* Correspondence: glvjinguo2005@163.com

Abstract: In this study, *Setaria viridis* was selected as the research object, the soil reinforcement mode of roots was analyzed, and the general mechanical model of soil reinforcement was proposed. The direct shear tests of root–soil composite and root tensile tests were carried out, and the relationship between the root additional cohesion and root depth was studied. Furthermore, numerical simulations were established to explore the variation law of shallow displacement and slope stability as a function of the root ratio. The results show that the effect of herbaceous plant roots on the soil was composed of material modification and root binding force on the soil. The shear strength improvement of the root–soil composite was mainly reflected by the increase in cohesion. Furthermore, the composite cohesion was positively correlated with the root content but negatively correlated with the water content. With the increase in root diameter, the tensile strength of the *Setaria viridis* root increased linearly, but its tensile strength decreased and showed a power relation. The greater the total cohesion of the root–soil composite layer, the smaller the total displacement and the higher the slope stability. Thus, the slope’s herbaceous vegetation could effectively control the deformation and slip of the shallow soil, which has good application value for reducing soil erosion in mining areas.

Keywords: herbaceous plant root system; root content; cohesion; internal friction angle; soil reinforcement and slip resistance



Citation: Lv, J.; Wang, W.; Dai, T.; Liu, B.; Liu, G. Experimental Study on the Effect of Soil Reinforcement and Slip Resistance on Shallow Slopes by Herbaceous Plant Root System.

Sustainability **2024**, *16*, 3475.
<https://doi.org/10.3390/su16083475>

Academic Editor: Adriano Sofò

Received: 24 February 2024

Revised: 17 April 2024

Accepted: 18 April 2024

Published: 21 April 2024



Copyright: © 2024 by the authors. Licensee MDPI, Basel, Switzerland. This article is an open access article distributed under the terms and conditions of the Creative Commons Attribution (CC BY) license (<https://creativecommons.org/licenses/by/4.0/>).

1. Introduction

A slope is one of the most common geological environments, which is naturally or artificially formed in human engineering practice [1]. With the increasing expansion of the production scale of open-pit coal mines in China, the original geological environment has been seriously damaged, such as the strata, groundwater, and surface vegetation, which has aggravated the occurrence of water loss, soil erosion, landslides, and other disasters.

With the gradual improvement of the ecological environment requirements, people are no longer satisfied with slope reinforcement without regard to the surrounding environment of the traditional slope protection, and thus, they are eager to find a way to meet the safety requirements of the project and beautify the slope protection mode.

For this reason, ecological slope protection techniques that consider the requirements of slope protection and the need for ecological protection are beginning to be widely used. Ecological slope protection is a means of reinforcing and protecting the shallow soil layers of slopes by planting plants on the slopes and utilizing the interaction between the plants and the rock and soil bodies. Compared with traditional slope protection methods, ecological slope protection has the characteristics of a simple construction process and low construction cost, which can not only achieve the purpose of stabilizing the slope but also help to restore the natural ecological environment.

Vegetation restoration and eco-reconstruction are critical measures to lower the damage to the surrounding ecology that has been affected by open-pit mining. Controlling the probability of shallow geological disasters on the slope will realize sustainable mining [2].

In recent years, the related studies of slope protection by vegetation have achieved rich results. In a study of a theoretical model of root–soil reinforcement, Endo and Tsuruta [3] carried out an in situ shear test on root soil; they pointed out that the Mohr–Coulomb theory can better explain the principle of root–soil reinforcement, and put forward the Mohr–Coulomb formula for calculating the additional cohesion of the root system. Based on the mechanical equilibrium equation, Wu et al. [4] established a vertical root–soil reinforcement model, which can simply evaluate the soil reinforcement effect of the root system. Gray and Leiser [5] established the inclined root–soil-fixing model based on Wu et al.'s work, which improved the practicability of the root–soil-fixing model. Pollen and Simon [6] introduced the fiber bundle theory model in fracture mechanics into the root system of the soil reinforcement theory and established the root additional cohesion evaluation model based on the root progressive failure theory, namely, the FBM model. Compared with Wu et al.'s model, the assumption of the FBM model is closer to the actual failure of a root–soil composite. Schwarz and Cohen [7] proposed a root enhancement model based on the FBM model, which can be called the RBM model. It more comprehensively considers the influence of the root tensile strength, length, and branching on the effect of root–soil consolidation, and the accuracy of the model was further improved.

In the practice of root reinforcement, Liu et al. [8] used FLAC3D to compare and analyze the reinforcement ability of two herbaceous plants, namely, *Poa pratensis* and *Suaeda glauca*, on a slope. The results showed that the failure modes of the slope were different with the different types of herbaceous plants. Ji and Yin [9] and Ji [10] used the PLAXIS3D finite element software to simulate the slope protection effect of roots at different growth times under rainfall conditions. They found that with the root growth, the soil consolidation effect was improved. Wu et al. [11] used finite element software to calculate the influence of cracks and root–soil gaps on the seepage field during rainfall. The results show that cracks and root–soil gaps can promote rainwater infiltration, reduce the strength of the soil itself, and weaken the soil-fixing effect of the root system. Wang et al. [12] carried out a large-scale direct shear test and numerical simulation of slope soil reinforced by roots with different lateral root inclination angles. They found that the front lateral roots can mobilize the surrounding soil to resist shear and enhance the effect of root reinforcement. Liu et al. [13] took the vetiver *zizanioides* root system as an example to derive a formula for the slope safety factor when the plant root angle was different. The accuracy of the formula was verified by a triaxial test. Hu et al. [14] conducted an unconfined compressive strength test on the shrub root–soil composite and found that the cohesion of the root–soil composite was significantly higher than that of the plain soil. Li et al. [15] used FLAC3D to analyze the effect of shrubs on the slope safety factor under different water content and found that shrubs have a good effect on enhancing slope stability.

However, plant slope protection is a long-term process [16,17], and the effectiveness of root slope protection is closely related to factors such as root distribution [18–20] and root density [21–23]. Therefore, further analysis is needed on the soil fixation mechanism of herbaceous plant roots.

To this end, this study combined field investigations, theoretical analyses, indoor experiments, and numerical simulations to research root fixation via mechanical modeling and root-containing soil shear characteristics via experimental analysis, as well as calculations for the cohesion force of the root system, the slope's shallow soil slip, and stability, to explore the mechanical role of a herbaceous plant root system on a fixation slope and the control effect on soil displacement. This will provide a new method for the quantitative evaluation of erosion, geologic landslides, and other hazards of shallow soils on open pit mine slopes.

2. Analysis of Soil Reinforcement and Slip Resistance by Herbaceous Plant Root System

2.1. Mechanical Analysis of Soil Reinforcement by Root System

In contrast to the root growth characteristics of woody plants, herbaceous plants have a root system that grows to a depth of less than 20 cm below the ground's surface and mostly have a fibrous root that is usually less than 1 mm in diameter. In the shallow soil of the slope, the fibrous roots of herbaceous plants are interspersed and entangled with each other, forming a root–soil composite that acts as the reinforcing effect and can effectively improve the ability of the soil to resist shear damage. It enhances the shear strength of the original soil and effectively restrains the deformation and movement of the shallow soil of the slope. The thicker root system of herbaceous plants can firmly lock the soil via anchoring, thereby enhancing the friction and the bonding effect between the roots and the soil; thus, this can provide anti-slip slope protection to a certain extent. Therefore, the action mode between the herbaceous root system and the soil is mainly reflected in the reinforcement modification and anchoring.

Soils with root interactions can be viewed as a root–soil composite. When the shallow root–soil composite of a slope undergoes critical instability, sliding occurs along the slip surface. The Mohr–Coulomb strength criterion can be used in conjunction with the reinforced soil principle to analyze the enhancement of the shear strength in the shallow soil of the slope that is generated by the root system of herbaceous plants. Thus, the root–soil composite shear strength should satisfy Equation (1):

$$\tau = \sigma \tan \varphi + c + \Delta\tau \quad (1)$$

where τ is the shear strength of the root–soil composite; σ is the normal stresses in the unrooted soil; φ is the angle of internal friction in the unrooted soil; c is the force of cohesion in the unrooted soil; and $\Delta\tau$ is the increase in shear strength resulting from the root–soil composite, which is called the total additional shear strength. The additional shear strength resulting from the root–soil composite can be composed of two parts. The first part is to consider the root–soil composite as a new material medium. The root system enhances the friction and bonding of the surrounding soil, which increases the angle of internal friction and cohesion. The second part is that the root system exerts a force on the soil to limit the shear deformation of the soil when shear deformation occurs in the shallow soil layer. However, when the shear deformation of the soil exceeds a certain limit, the root system will be pulled off, which can be viewed as the additional shear strength produced by the action of the root tension. Thus, the additional shear strength of the root–soil composite can be written as Equation (2):

$$\Delta\tau = \Delta\tau_m + \Delta\tau_T \quad (2)$$

where $\Delta\tau_m$ is the additional shear strength generated by the new material and $\Delta\tau_T$ is the additional shear strength generated by the root tension.

The additional shear strength of the new root–soil composite material is shown in Equation (3), where the additional shear strength, the increase in the internal friction angle, and the increase in cohesion can be obtained by a shear test:

$$\Delta\tau_m = \sigma[\tan(\varphi + \Delta\varphi_m) - \tan \varphi] + \Delta c_m \quad (3)$$

where $\Delta\varphi_m$ is the angle of internal friction added to the root–soil composite and Δc_m is the cohesion added to the root–soil composite.

In this study, the FBM model [24–26] was utilized to quantitatively describe the additional shear strength resulting from the reinforcement of the root system, as shown in Equation (4), where the tensile strength of the root system can be obtained from a single root tensile test:

$$\Delta\tau_T = \Delta c_T = \max(1.2\sigma_i \sum R_i) \quad (i = 1, 2, \dots, n) \quad (4)$$

where σ_i is the root tensile strength and R_i is the root area ratio.

2.2. Mechanical Analysis of Slip Resistance by Root System

On a slope with a slope angle of α , an arbitrary micro-segment dl of the primary or coarse root at a depth z from the surface is taken. The coefficient of static friction between the root and the soil is μ , γ is the soil volumetric weight, and the inclination angle of the micro-segment root extension is θ , as shown in Figure 1.

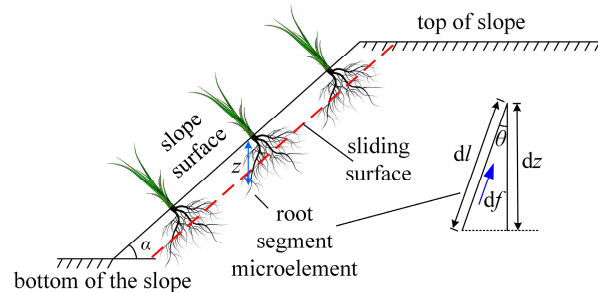


Figure 1. Schematic diagram of the anti-slip of herbaceous plant roots.

When the shallow soil of the slope slides along the shear face boundary, the maximum static friction df applied to the root of the microsection can be calculated using

$$df = \mu \gamma z \cdot 2\pi r \cdot dl \quad (5)$$

From Equation (5), the component of the maximum static friction force on the root system in the vertical direction is independent of θ . If the distribution function of the average radius of the entire root system along the depth z direction is $D(z)$, and the distribution function of the number of roots along the depth z direction is $N(z)$, then the maximum static friction of the root system within the depth of H in the vertical direction component F_z is

$$F_z = 2\pi \gamma \tan(\varphi + \Delta\varphi_m) \int_0^H D(z) \cdot N(z) \cdot z dz \quad (6)$$

where $\mu = \tan(\varphi + \Delta\varphi_m)$ is the coefficient of static friction and $\varphi + \Delta\varphi_m$ is the angle of internal friction of the root–soil composite. The frictional resistance component F_α provided by the root system along the slope angle is

$$F_\alpha = F_z \sin \alpha \quad (7)$$

If critically unstable sliding occurs along a weak surface (slip surface) and the direction of the residual thrust is parallel to the slope, the residual thrust P_s of the sliding body can be found using

$$P_s = G \sin \alpha - G \cos \alpha \tan \varphi - c A_s \quad (8)$$

If the stability of a shallow slope soil is maintained, then it satisfies

$$F_\alpha - P_s \geq 0 \text{ or } F_\alpha / P_s \geq 1 \quad (9)$$

3. Experimental Study on Anti-Shear Performance of Herbaceous Plant Root–Soil Composites

3.1. Overview of the Study Area

The herbaceous plant sample collection site was in the open pit of Haizhou, Fuxin City, Liaoning Province, on a slope about 50 m above ground level, as shown in Figure 2. The mine is located at latitude $42^\circ 01' N$ and longitude $121^\circ 40' E$. The temperature changes throughout the year, where it is windy, with little rain, and dry; the highest temperature in summer can reach $40.6^\circ C$, the lowest temperature in winter is $-28.4^\circ C$, the average annual temperature is $7.8^\circ C$, the average annual precipitation is 519.3 mm, and the number

of hours of sunshine is 2630 h per year, and thus, this place is considered a semi-arid region [27].

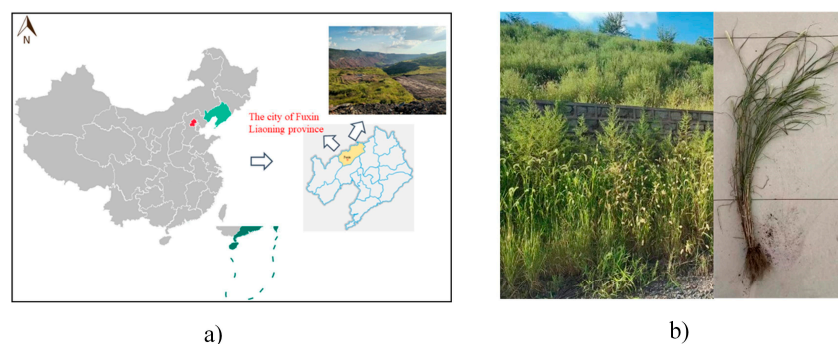


Figure 2. Overview of the sampling site: (a) study area; (b) research object.

The Haizhou open-pit mine has formed a huge pit covering an area of about 7.02 km² after a long period of mining. It is rectangular in shape, trending from southwest to northeast, with a ground elevation of 130~170 m, a pit elevation of 170~180 m, and a mining depth of 350 m. The final slope angles of the southern and northern slopes of the mine are about 38° and 18~20°, respectively.

At present, the Haizhou open-pit mine is closed, and the ecological environment of the slopes of the pit has been damaged to a certain extent. The existing vegetation is mainly *Setaria viridis*, *Arundinella hirta* Tanaka, and Herb of Common Crabgrass. Among them, *Setaria viridis* is the most common in the Haizhou mining area, with a large number and lush growth. Therefore, sufficient experimental materials could be obtained, and the main research object was the root system of *Setaria viridis*.

3.2. Specimen Preparation

According to the growth pattern of herbaceous plant roots, the diameter and weight of roots in soil will change significantly with the increase in depth. Hence, the root ratio index was used to characterize the root–soil composite and to obtain the root–soil composite percentage at different depths. The root ratio of remodeled soils was designed according to the actual root ratio of shallow soils in the Haizhou open-pit mine slope. The root ratio in the soil was calculated using Equation (10):

$$\eta = \frac{m_1}{m_2} \times 100\% \quad (10)$$

where η denotes the root ratio of the soil, %; m_1 denotes the dry weight of the root system, g; and m_2 denotes the dry weight of the soil, g.

In this study, the root ratios of the soil at different depths were measured in the field using the sectioning method. A 10 cm × 10 cm area was delineated. Then, four horizontal sections were dug for each plant starting from 2 cm below the slope surface, with each section 2 cm apart in the vertical direction, and all the roots within the top and bottom neighboring two sections were dug out. The roots of five *Setaria viridis* were dug in the same way. The dry density of the soil was measured and then multiplied by the volume of each layer of soil to obtain the weight of each soil layer. The natural root ratio of the soil at different depths was calculated using Equation (10). The average value of the root ratios of the five *Setaria viridis* plants under the same soil depth was taken as the statistical result of the root ratio at this depth. Actual measurements found that the *Setaria viridis* root system was negligible when the soil depths were greater than 8 cm, with almost zero content in the soil. Therefore, only the root ratios of soil depths in the range of 0 to 8 cm were counted in this experiment. The average root ratio of the root–soil composite at different depths is shown in Table 1.

Table 1. Root system statistics.

Soil Depth (cm)	Average Root Content (%)
0~2	0.373
2~4	0.289
4~6	0.193
6~8	0.097

The root ratio of the *Setaria viridis* root–soil composite decreased gradually with the increase in root growth depth. Its root system reached the maximum root ratio in the depth range of 0–2 cm, with a maximum value of 0.373%. Based on the above statistical results, the root ratio of the root–soil composite in the direct shear test was set to 0.4, 0.3, 0.2, 0.1, and 0%, respectively, which corresponded to characterizing the root content of the soil layer at depths of 0–2, 2–4, 4–6, 6–8, and >8 cm.

Through the determination of the water content of the original soil with roots and soil without roots taken from the slopes of the Haizhou open-pit mine, it was found that the water contents of the two were almost the same, which were around 13%, indicating that the addition of the roots had a minimal effect on the original water content of the soil. Thus, the test could be carried out by adding roots directly to the plain soil. Combined with the measured values of the water content of the in situ soil, the water contents of the four root–soil composite specimens mentioned above were controlled at 9, 11, and 13%.

The configured root–soil composite specimens were sealed, compacted, and left to rest for 12 h. A total of 180 sets of ring knife samples were prepared, and all specimens underwent the direct shear test within 3 days of sampling to prevent the roots from decaying and deteriorating, and thus, losing their biological activity.

All sampling and test methods were in accordance with the Standard for geotechnical testing method (GB/T50123-2019) [28].

3.3. Direct Shear of Root–Soil Composites

The direct shear test used an STSJ-5A intelligent electric quadruple direct shear apparatus, and the test rate was set to 0.8 mm/min under normal stress conditions of 100, 200, 300, and 400 kPa (Figure 3). The shear test was performed, and the displacement meter was read. Measurements were recorded every 10 s, and each sample was cut for 5 min. The inner diameter of the ring cutter used in the test was 61.8 mm, the cross-sectional area was 30 cm², and the stress ring coefficient was 3 N/0.01 mm. The formula for calculating the shear stress of the soil could be calculated using

$$\tau = \frac{10CR}{A} \quad (11)$$

where C is the stress ring coefficient, N/0.01 mm; R is the stress ring reading, mm; and A is the cross-sectional area of the shear sample, cm².



Figure 3. Straight shear specimens and equipment: (a) root-bearing soil ring cutter sample; (b) STSJ-5A intelligent electric instrument with four straight shears.

The shear stress and shear displacement curves of the root–soil composite were drawn for 9, 11, and 13% water contents and 0.1, 0.2, 0.3, and 0.4% root contents. Because the shear stress and shear displacement curve characteristics of the samples under three water content conditions were similar, only the curve found when the water content was 13% is displayed (Figure 4).

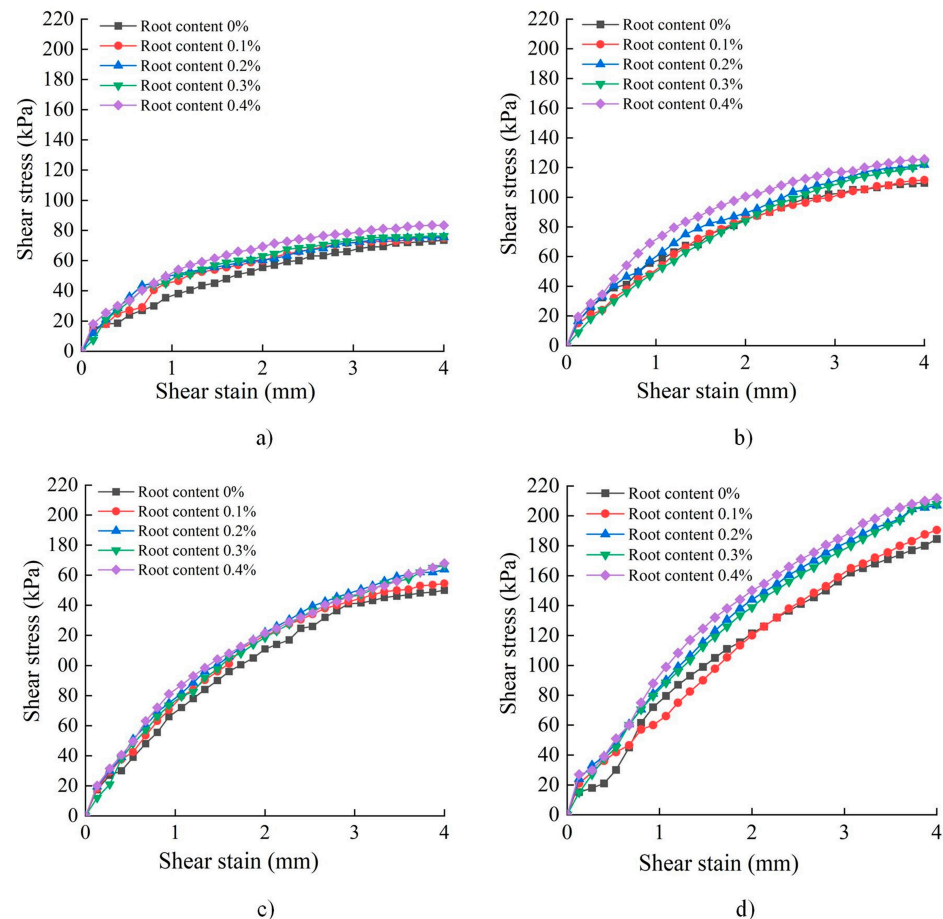


Figure 4. Shear displacement–shear stress relationship of the root–soil composite with 13% water content under different normal stresses: (a) $\sigma = 100$ kPa; (b) $\sigma = 200$ kPa; (c) $\sigma = 300$ kPa; (d) $\sigma = 400$ kPa.

The *Setaria viridis* root–soil composite shear stress tended to increase nonlinearly with increasing shear displacement. The shear stress growth rate was faster in the early stage, and the later stage slowed down and finally reached the maximum shear stress. Then, shear failure occurred, and the maximum shear stress at this time was called the shear strength. For a certain moisture content, the shear strength of the root–soil composite sample increased with the increase in the normal stresses. This was due to the increase in normal stresses, which made the frictional resistance between the root and the soil increase, which could inhibit the shear deformation of the soil to a certain extent, and thus, improve the shear strength of the soil.

The maximum shear stress of the specimen under different normal stresses was recorded, that is, the shear strength under the normal stresses. According to the Mohr–Coulomb strength criterion, the linear relationship between the normal stresses and shear strength was established, and the fitting function between the normal stresses and shear strength was obtained to calculate the cohesion c and internal friction angle φ of the root–soil composite (Table 2).

Table 2. Cohesion and internal friction angle results for the pure soil and root–soil composite.

Type	Moisture Content (%)	Rooting Rate (%)	Root Growth Depth (cm)	Fitting Equation	R ²	Internal Friction Angle (°)	Cohesion (kPa)
Pure soil	9	0	0	$\tau_{\max} = 0.4164\sigma + 22.8$	0.98331	24.77	22.8
	11	0	0	$\tau_{\max} = 0.4068\sigma + 42.6$	0.96705	22.14	42.6
	13	0	0	$\tau_{\max} = 0.3795\sigma + 36.0$	0.98870	20.78	36.0
<i>Setaria viridis</i>	9	0.1	6~8	$\tau_{\max} = 0.3924\sigma + 48.0$	0.9938	21.42	48.0
		0.2	4~6	$\tau_{\max} = 0.3861\sigma + 57.5$	0.9454	21.11	57.5
		0.3	2~4	$\tau_{\max} = 0.3843\sigma + 59.1$	0.94175	21.02	59.1
		0.4	0~2	$\tau_{\max} = 0.4011\sigma + 60.1$	0.94282	21.86	60.1
	11	0.1	6~8	$\tau_{\max} = 0.3862\sigma + 43.2$	0.99295	21.12	43.2
		0.2	4~6	$\tau_{\max} = 0.3931\sigma + 44.7$	0.98171	21.46	44.7
		0.3	2~4	$\tau_{\max} = 0.4317\sigma + 44.1$	0.99851	23.35	44.1
		0.4	0~2	$\tau_{\max} = 0.4352\sigma + 46.5$	0.99441	23.52	46.5
	13	0.1	6~8	$\tau_{\max} = 0.3804\sigma + 38.6$	0.99699	20.82	38.6
		0.2	4~6	$\tau_{\max} = 0.4263\sigma + 36.3$	0.99996	23.09	36.3
		0.3	2~4	$\tau_{\max} = 0.4287\sigma + 37.1$	0.99978	23.20	37.1
		0.4	0~2	$\tau_{\max} = 0.4257\sigma + 41.0$	0.99981	23.06	41.0

According to Table 2, the relationship curves for the root content, cohesion, and internal friction angle of the root–soil composite were drawn (Figure 5). Figure 5a shows that under three different water content conditions, the cohesion of the *Setaria viridis* root–soil composite generally increased with the increase in root content when the root content was in the range of 0~0.4%. For example, when the water content was 9%, the root–soil composite cohesions at 0.1, 0.2, 0.3, and 0.4% root ratios increased by 110.5, 152.2, 159.2, and 163.6%, respectively, compared with those of the plain soil. Thus, the cohesion of the root–soil composite decreased with the increase in the water content in general. The addition of roots significantly improved the shear strength of the soil.

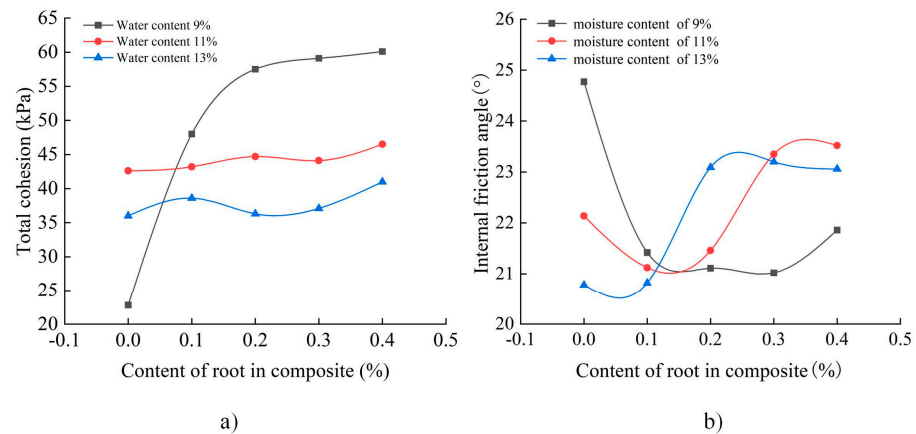
**Figure 5.** Relationship between strength parameters and the root content in root–soil composite: (a) total cohesion; (b) internal friction angle.

Figure 5b shows that the internal friction angle of the *Setaria viridis* root–soil composite had a decreasing and then increasing trend with the increase in root ratio at a 9% water content. When the moisture contents were 11 and 13%, the internal friction angle increased with the increase in root content. The highest increase in the angle of internal friction was found in two places. For the 11% moisture content, the angle of internal friction of the 0.3% root ratio composite was 13.5% higher than the 0.2% root ratio. For the moisture content of 13%, the angle of internal friction of the 0.2% root ratio composite was 10.9% higher than the 0.1% root ratio. Overall, the trends of the internal friction angles of root–soil composites

at different water contents were significantly different, suggesting that the water content had a strong influence on the internal friction angle of the root–soil composites. However, there was relative uncertainty about the impact of their increase or decrease.

In summary, it was shown that the variation in the angle of internal friction was also an important indicator of the shear strength of the soil. Based on the influence degree of the change in cohesion and internal friction angle of the root–soil composite on shear strength, the influence degree of the roots on soil cohesion was greater than that of the internal friction angle. Thus, the improvement of shear strength of the root–soil composite was mainly reflected in the cohesion improvement, followed by the internal friction angle.

4. Root System Tensile Test of a Herbaceous Plant and Its Additional Cohesion Characteristics

4.1. Root Area Determination Method

The root area ratio R is defined as the ratio of the total cross-sectional area of all roots to the shear area of soil within a certain range of soil depth. It is an important parameter to characterize the distribution characteristics of roots in the vertical plane of soil and evaluate the root consolidation capacity.

The root area ratios at different depths were calculated using Equation (12):

$$R = \sum_{i=1}^N \frac{\pi d_i^2}{4A} \quad (12)$$

where R is the root area ratio; N is the number of roots; d_i is the diameter of the i th root, mm; and A is the area of the soil profile, mm².

Five *Setaria viridis* plants were selected in the study area, and the root area ratios at different depths were calculated and averaged. The calculation results are shown in Table 3.

Table 3. Root area ratio results.

Soil Depth (cm)	Root Area Ratio (10 ^{−4})
0~2	3.5
2~4	2.3
4~6	0.9
6~8	0

4.2. Root System Tensile Test of a Herbaceous Plant

To more easily measure the root-pulling force, a simple device was made for root pulling. The device consisted of three parts: the fixing frame, the clamp, and the sandbag. The roots were fixed perpendicular to the horizontal plane to ensure that the roots were subjected to an axial load. The lower part of the root system was continuously loaded through the sandbag until the root system was broken. The weight of the sandbag was weighed as the tensile strength of the root system. The tensile strength of the root was recorded only when the root was broken in the middle or near the middle part, and the root diameter at the fracture was measured. The tensile strength of the root was calculated according to Equation (13):

$$\sigma = \frac{4T_{\max}}{\pi d^2} \quad (13)$$

where σ is the root tensile strength, MPa; T_{\max} is the tensile force at the fracture, N; and d is the average root diameter, mm.

4.3. Relationship between Tensile Strength and Diameter

The *Setaria viridis* root samples were selected at different locations in the study area; then, we conducted the root axial tensile test. The anti-tensile force and tensile strength of the roots of 10 *Setaria viridis* plants were obtained and fitted. Anti-tensile force refers to the maximum tensile stress in the root length direction. The results are shown in Figure 6.

The anti-tensile force of the *Setaria viridis* plant root system increased with increasing root diameter, and the linear relationship was significant. The tensile strength of the root system decreased with increasing diameter, and there was a clear exponential relationship with the root diameter.

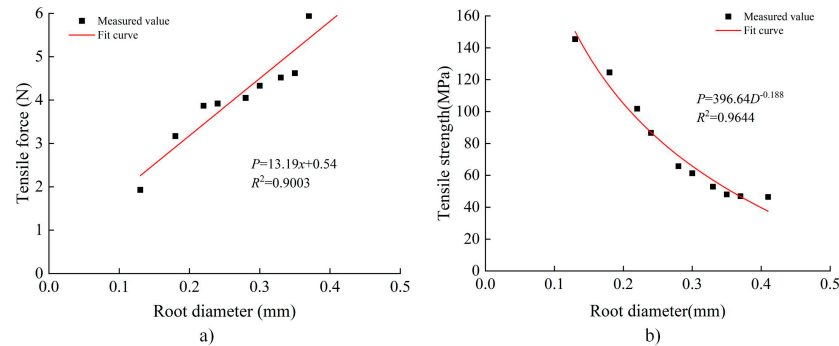


Figure 6. Relationship between tensile parameters and diameter of root: (a) tensile force at fracture; (b) tensile strength.

Combined with the development characteristics of roots, the root diameters at different depths were different and generally decreased gradually along the growth direction. However, the decrease in root diameter reduced the anti-tensile force of the roots, which affected the reinforcement and anti-sliding effect of herbaceous plant roots on the slope soil. This shows that the effect of soil reinforcement and slope protection of herbaceous plant roots changed with the change in soil depth.

4.4. Calculation of Root Additional Cohesion and Total Additional Cohesion

Under the combined conditions of 9, 11, and 13% moisture contents and 0, 0.1, 0.2, 0.3, and 0.4% root contents, combined with the cohesion obtained from the direct shear test of the root–soil composite, the additional cohesion of the root–soil composite could be calculated under the above combinations. By measuring the root area ratio and root tensile strength, the FBM model was used to calculate the additional cohesion of roots under different root content conditions. The sum of the additional cohesion of the composite material and the additional cohesion of the root system was used to characterize the total additional cohesion after the root system acted on the soil. The calculation results are shown in Table 4.

Table 4. Total additional cohesion results.

Moisture Content (%)	Depth (cm)	Root Content (%)	Additional Cohesion of Composite Materials (kPa)	Additional Root Cohesion (kPa)	Total Additional Cohesion (kPa)
9	0~2	0.4	37	5.07	42.07
9	2~4	0.3	36.43	3.33	39.76
9	4~6	0.2	34.02	1.3	35.32
9	6~8	0.1	23.98	0.29	24.27
9	>8	0	0	0	0
11	0~2	0.4	3.42	5.07	8.49
11	2~4	0.3	2.49	3.33	5.82
11	4~6	0.2	1.56	1.3	2.86
11	6~8	0.1	0.63	0.29	0.92
11	>8	0	0	0	0
13	0~2	0.4	4.99	5.07	9.97
13	2~4	0.3	1.05	3.33	4.38
13	4~6	0.2	0.26	1.3	1.56
13	6~8	0.1	2.62	0.29	2.91
13	>8	0	0	0	0

With a 9% moisture content and a 0.4% root content, the total additional cohesion of *Setaria viridis* reached the maximum, namely, 42.07 kPa. With an 11% moisture content and a 0.4% root content, the total additional cohesion of *Setaria viridis* reached 8.49 kPa. With a 13% moisture content and a 0.4% root content, the total additional cohesion of *Setaria viridis* reached 9.97 kPa.

Overall, the total additional cohesion decreased with the increase in moisture content. The main reason was that when the moisture content reached a certain level, water had a certain weakening effect on the shear strength of the root–soil composite. Under the 9, 11, and 13% moisture content conditions, the total additional cohesion under the action of *Setaria viridis* roots increased with the increase in root content.

5. Numerical Simulation of Shallow Slope Stability under the Effect of a Herbaceous Plant Root System

In order to quantify the effect of the herbaceous plant roots on slope stability, taking the geological survey of the north slope of Haizhou open-pit mine in Fuxin as a reference, we undertook two approaches. First, based on FLAC3D 6.0 software, we established a three-dimensional numerical model of the slope to analyze the influence of herbaceous plant roots on the displacement of shallow soil in the slope. Second, based on GEO-SLOPE 2018 software, we calculated the slope safety factor by considering the effect of the plant roots and analyzed the influence of herbaceous plant roots on slope stability.

5.1. Numerical Model Establishment

This study was based on the northern slope of the Haizhou open-pit mine. A simplified three-dimensional numerical model was established by using slope step sizes between $E10^{-5}$ and $E10^{-6}$ for the northern slope of the Haizhou open-pit mine. The model was 7.5 m high, 25.9 m long, and 20 m wide. The level of the northern slope was about 150~170 m, and the slope angle was about 20° [29]. According to the engineering geological report of the Haizhou open-pit mine, the surface layer of the mining area is the Quaternary flood impact loose layer. According to the results of the root tensile and laboratory direct shear tests, the soil consolidation effects of roots at different soil depths were different. To simulate the soil consolidation effects of the root system more realistically, the soil 8 cm below the surface was layered, and the thickness of each layer was 2 cm.

The y-direction displacement constraint was set at the front and back of the model, the x-direction displacement was limited on the left and right sides, and the z-direction constraint was limited on the bottom surface. The slope top, slope bottom, and slope surface were free surfaces, and the model adopted the Mohr–Coulomb yield criterion. The monitoring points were arranged along the slope. The horizontal distance of each measuring point was 0.3 m. A row of measuring points was arranged vertically downward from the slope surface at intervals of 2 cm, and 47 measuring points were arranged in each row, which monitored the displacement characteristics of the root–soil composite layer of the slope at different depths. The section size and layout of the model are shown in Figure 7.

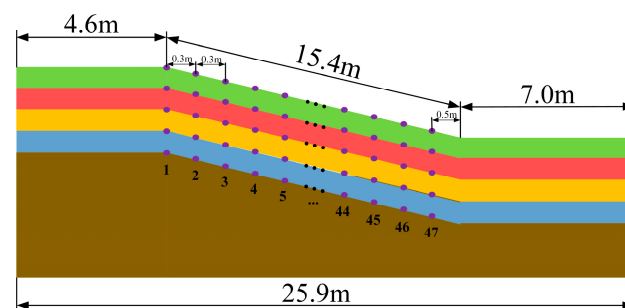


Figure 7. Schematic diagram of model section size and monitoring point layout.

Four schemes were set up in the numerical simulation. Scheme 1 was the plain soil slope, that is, the root content was 0, and the slope was the Quaternary flood impact loose layer; schemes 2, 3, and 4 corresponded to the root–soil composite layers of the slope under the 9, 11 and 13% water contents, and the root contents from top to bottom were 0.4, 0.3, 0.2, and 0.1%, respectively.

Due to the differences in the mechanical properties between the remolded soil obtained from the laboratory direct shear tests and the undisturbed soil of the open-pit mine slope, we took the following measures. To make the simulation results more realistic, we used the physical and mechanical parameters of undisturbed soil from the Haizhou open-pit mine area, which were combined with the total additional cohesion of the root–soil composite obtained from the laboratory tests. Thus, a fitting function between the total additional cohesion and the root content was established, and the total additional cohesion at any given root content could be obtained. Under the same root rate, the cohesion of the undisturbed soil was superimposed in the mining area, which provided the total cohesion after a conversion. The conversion method of the internal friction angle was similar to that of the cohesion. The increase in the internal friction angle was fitted with the root ratio, and the increase in the internal friction angle under different root ratios was calculated. Under the same root ratio, the total internal friction angle under a certain root ratio was obtained by adding it to the internal friction angle of undisturbed soil. The physical and mechanical properties of the soil layer in the study area are shown in Table 5, which have been obtained from reference [30], and the total cohesion and total internal friction angle of the soil layer under the action of the converted roots are shown in Table 6.

Table 5. Physical and mechanical parameters of an unconsolidated formation (based on [30]).

Density (kg/m ³)	Bulk Modulus (MPa)	Shear Modulus (MPa)	Poisson's Ratio (-)	Cohesion (kPa)	Angle of Internal Friction (°)
1410	2.22	1.67	0.2	10.5	20

Table 6. Soil cohesions and internal friction angles of different schemes.

Scheme	Soil Depth (cm)	Root Content (%)	Moisture Content (%)	Total Cohesion (kPa)	Total Internal Friction Angle (°)
Scheme 1	0~2	0	0	10.5	20
	2~4	0		10.5	20
	4~6	0		10.5	20
	6~8	0		10.5	20
Scheme 2	0~2	0.4	9	54.54	17.05
	2~4	0.3		48.75	16.35
	4~6	0.2		42.97	16.23
	6~8	0.1		37.18	16.69
Scheme 3	0~2	0.4	11	18.87	21.59
	2~4	0.3		16.31	20.68
	4~6	0.2		13.74	19.77
	6~8	0.1		11.17	18.86
Scheme 4	0~2	0.4	13	20.54	22.35
	2~4	0.3		14.67	22.35
	4~6	0.2		12.27	22.34
	6~8	0.1		13.34	21.38

5.2. Deformation Law of Shallow Soil under the Effect of a Herbaceous Plant Root System

Figure 8 shows that the displacement magnitude at about 2 m from the top of the slope was the smallest; after 2 m, the displacement magnitude of the slope in the shallow depth of 8 cm increased rapidly with the increase in the distance from the top of the slope; when the distance from the top of the slope was about 8 m, the total displacement reached the maximum; after 8 m, the total displacement decreased slowly with the distance

from the top of the slope, that is, the total displacement near the foot of the slope was smaller. The soil displacements of the rooted slopes were smaller than those of the unrooted slopes in scheme 1, indicating that rooting was effective in reducing the soil displacements. Comparing schemes 2, 3, and 4 under the same root content conditions, the shallow soil displacement of the slope showed an increasing and then decreasing trend with the increase in moisture content.

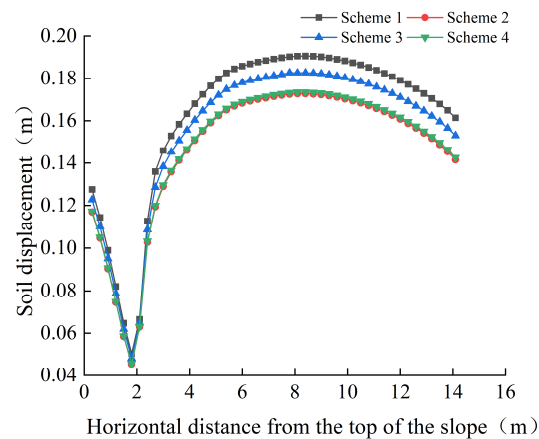


Figure 8. Total displacement of monitoring points at a depth of 2 cm in the slope soil layer.

5.3. Influence Pattern of Slope Stability Due to a Herbaceous Plant Root System

Consistent with the physico-mechanical parameters chosen for the FLAC3D 6.0 software, the GEO-SLOPE 2018 software was used to calculate the slope stability for the four schemes. To calculate more accurate results, the number of calculation iterations was set to 3000, with an acceptable safety factor error of 0.001. The analytical method was the Morganstein–Price (M-P) method, and the bar function was a half-sine function. The shear properties of the soil conformed to the Moore–Coulomb criterion, with horizontal displacements limited on the left and right sides of the model; vertical displacements were limited at the bottom of the model; and the top of the slope, the bottom of the slope, and the slope surface were free surfaces, with only the self-weight considered, and there was no dynamic disturbance. The model dimensions are shown in Figure 9.

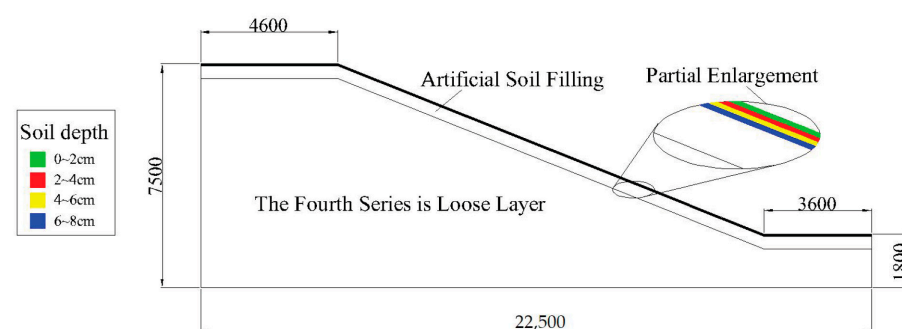


Figure 9. Model dimensions and soil structure.

Under the 9, 11, and 13% moisture contents, different rooting rates were set, and the specific schemes are detailed in Table 6. The slope stability coefficients under different schemes were calculated and are shown in Figure 10.

Among them, the slope stability coefficient of scheme 1 was the smallest at 2.301, while the stability coefficients of schemes 2–4 were 2.321, 2.306, and 2.306, respectively. Comparing schemes 2–4 shows that the addition of the root system enhanced the shear strength of the slope soil, thereby improving the stability of the slope. The overall stability of the slope decreased with the increase in soil moisture content under the same root

content, and the higher the root density, the greater the shear strength of the slope soil and the higher the stability.

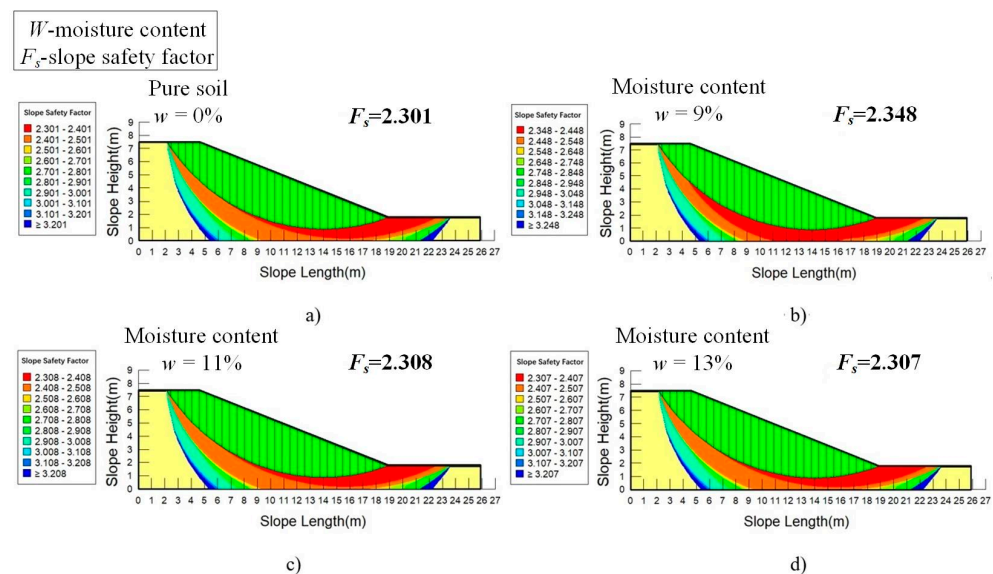


Figure 10. Calculation slope stability coefficients of different schemes: (a) scheme 1—pure soil; (b) scheme 2—the soil–root composite with 9% moisture content; (c) scheme 3—the soil–root composite with 11% moisture content; (d) scheme 4—the soil–root composite with 13% moisture content.

6. Discussion

In this study, based on the Mohr–Coulomb theory, combined with the reinforced soil theory and the FBM model, a mechanical model of root reinforcement and modification was established to evaluate the effect of root reinforcement on herbaceous plants. Different from the previous mechanical model, the model not only considered the mechanical effect of the root system on the soil but also considered the shear mechanical properties of the new material formed by the root–soil composite, which overcame the issue where the previous model only paid attention to the mechanical properties of the root system and ignored the shear capacity of the soil itself; therefore, the model had higher accuracy.

The tests used in the model were all indoor tests, which provides a solution for projects that cannot carry out in situ shear tests due to environmental factors and reduces the influence of environmental factors on the test results.

Based on the laboratory test of the root–soil complex and the calculation results of the slope stability, the conclusions obtained in this study were consistent with the existing results [30–33]. The results indicated that the herbaceous plant root system had an enhanced effect on the shear strength and stability of the mine slope. Furthermore, the effectiveness of the mechanical model of root–soil reinforcement proposed in this study and the rationality of the obtained material’s mechanical parameters were further illustrated. By using this model to estimate and evaluate the soil-fixing ability and effect of herbaceous plant roots, it can select suitable herbaceous plants for ecological restoration of open-pit mines and has certain reference significance for the prediction of shallow slope stability in mining areas.

In this study, the M–P method was used to calculate the stability of the slope, and the influence of herbaceous roots on the stability of the slope was quantified by comparing the stability coefficients of the slope with roots and the slope without roots. However, it is worth noting that slope stability analysis is a comprehensive evaluation and analysis process. Due to incomplete engineering data or inconsistent evaluation standards of slope stability, it is difficult to accurately evaluate the stability of a slope by relying only on deterministic analysis methods. In recent years, relevant researchers have introduced the uncertainty method and the uncertainty analysis method, which combines the determined parameters with the prediction of the failure probability in slope stability calculations [34–36]. The

combination of quantitative calculations and qualitative evaluation can be better applied to engineering practice. Combining the deterministic analysis method with the uncertainty analysis method to evaluate the slope stability will be one of the future research directions of this research group.

This study only considered the most common Bermuda grass in the Haizhou open-pit mine, which is a fibrous root herb. In fact, there are straight-root plants in the mining area. It was found that there may be differences in the soil consolidation mechanism of different roots. Therefore, the research and analysis of the influence of different root types on the stability of the slope will be the follow-up research direction of this study. At the same time, the growth status of the root system was affected by factors such as time, soil organic matter content, nutrients, and climate. Hence, the soil-fixing effect of the same plant in different periods and different geographical conditions may still be different. If the functional relationship between the mechanical properties of the root system and these factors can be established, the influence of these factors on the soil-fixing effect of the root system can be quantified, which will be the focus of the next step of this research direction.

7. Conclusions

- (1) For herbaceous plants with a fine root diameter and shallow growth depth, the reinforced soil of a root–soil composite can be divided into a linear superposition of two parts. First, the root–soil composite is regarded as a new material medium, which increases the internal friction angle and cohesion of the original soil and improves the shear strength. The second is the effect of the root force on the soil, that is, the additional shear strength generated by the root tension effect. In this way, a mechanical model of root-modified soil consolidation is proposed, which can be used to evaluate and analyze the root consolidation effect in herbaceous plants.
- (2) The root–soil cohesion and shear strength increased with the increase in root content and decreased with the increase in moisture content. The combination of roots and soil significantly improved the plain soil cohesion, and its change was an important index that affected the shear strength of the soil. The improvement of the shear strength of the root–soil composite was mainly reflected in the increase in cohesion, and the internal friction angle had little effect on the shear strength. The tensile strength of the roots increased with the increase in the root diameter and showed a linear relationship. The root–soil composite’s tensile strength decreased with the increase in diameter, showing an exponential relationship. The root area ratio decreased with the increase in soil depth and showed a quadratic relationship with soil depth. The additional cohesion of roots decreased with the increase in soil depth. Under the 9, 11, and 13% moisture contents, the total additional cohesion decreased with the increase in moisture content and increased with the increase in root content.
- (3) The total displacement of the root–soil composite layer of the slope decreased with the increase in the root ratio. The slope stability increased with the increase in the root content and generally decreased with the increase in water content. Herbaceous vegetation on the slope could effectively control the slip of shallow soil and improve the overall stability of the slope. This has certain reference significance for the prediction of soil erosion and slope stability in the shallow slope of the mining area and has good application value.

Author Contributions: Methodology, J.L.; data curation, T.D.; writing—original draft, W.W.; visualization, B.L.; funding acquisition, G.L. All authors have read and agreed to the published version of the manuscript.

Funding: This research received no external funding.

Institutional Review Board Statement: Not applicable.

Informed Consent Statement: Not applicable.

Data Availability Statement: The data that support the findings of this study are available from the corresponding author upon reasonable request.

Conflicts of Interest: The authors declare that they have no known competing financial interests or personal relationships that could have appeared to influence the work reported in this paper.

References

- Zhou, Y. Study on mechanism of Soil Rand slope protection technology. *China Univ. Geosci.* **2010**, *5*, 1.
- Xiao, D.; Bi, Y.; Yu, L. Key Climate Factors in Species Introduction for Ecological Reconstruction of the Dump Site of Shenhua Baorixile Open-pit Mining. *J. South China Norm. Univ.* **2021**, *53*, 73–82. [[CrossRef](#)]
- Endo, T.; Tsuruta, T. The effect of tree roots upon the shearing strength of soil. *Tokyo For. Exp. Stn.* **1969**, *16*, 168–179.
- Wu, T.H.; Mckinell, W.P.; Swanston, D.N. Strength of tree roots and landslides on Prince of Wales Island, Alaska. *Can. Geotech. J.* **1979**, *16*, 19–33. [[CrossRef](#)]
- Gray, D.H.; Leiser, A.T. *Biotechnical Slope Protection and Erosion Control*; Van Nostrand Reinhold Company Inc.: New York, NY, USA, 1982.
- Pollen, N.; Simon, A. Estimating the mechanical effects of riparian vegetation on streambank stability using a fiber bundle model. *Water Resour. Res.* **2005**, *41*, 1–11. [[CrossRef](#)]
- Schwarz, M.; Cohen, D. Spatial characterization of root reinforcement at stand scale: Theory and case study. *Geomorphology* **2012**, *171–172*, 190–200. [[CrossRef](#)]
- Liu, X.; Hao, G.; Yu, B. Distribution characteristics of two kinds of plant roots and their effects on surface reinforcement of Open-pit mine slope. *J. Yangtze River Sci. Res. Inst.* **2022**, *39*, 96–101. [[CrossRef](#)]
- Ji, L.; Yin, P. Influence of different root growth stages on the slope anti-erosion performance. *J. Cent. South Univ. For. Technol.* **2020**, *40*, 144–150,178.
- Ji, X.L. Numerical simulation of root distribution on the slope protection. *China Sci.* **2020**, *15*, 652–656.
- Wu, M.; Zhou, C.; Wang, L. Numerical simulation of the influence of roots and fissures on hydraulic and mechanical characteristics of the soil. *Rock Soil Mech.* **2019**, *40*, 519–526+534. [[CrossRef](#)]
- Wang, Y.; Wu, M.; Zhou, C. Direct shear test and numerical simulation of combined root reinforcement of slope soil. *J. Geotech. Eng.* **2020**, *42*, 177–182. [[CrossRef](#)]
- Liu, J. Effect of root system distribution on slope stability. *Pearl River* **2020**, *41*, 140–145.
- Hu, X.; Brierley, G.; Zhu, H. An Exploratory Analysis of Vegetation Strategies to Reduce Shallow Landslide Activity on Loess Hillslopes, Northeast Qinghai-Tibet Plateau, China. *J. Mt. Sci.* **2013**, *10*, 668–686. [[CrossRef](#)]
- Li, J.; Wang, X.; Jia, H.; Liu, Y.; Zhao, Y.; Shi, C.; Zhang, F. Assessing the soil moisture effects of planted vegetation on slope stability in shallow landslide-prone areas. *J. Soils Sediments* **2021**, *21*, 2551–2565. [[CrossRef](#)]
- Dumlao, M.R.; Ramanarivo, S.; Goyal, V.; DeJong, J.T.; Waller, J.; Silk, W.K. The role of root development of *Avena fatua* in conferring soil strength. *Am. J. Bot.* **2015**, *102*, 1050–1060. [[CrossRef](#)] [[PubMed](#)]
- Wang, B.; Wang, S. Shear Strength Analysis and Slope Stability Study of Straight Root Herbaceous Root Soil Composite. *Appl. Sci.* **2023**, *13*, 12632. [[CrossRef](#)]
- Liu, S.; Li, J.; Ji, X.; Fang, Y. Influence of root distribution patterns on soil dynamic characteristics. *Sci. Rep.* **2022**, *12*, 13448. [[CrossRef](#)] [[PubMed](#)]
- Cao, T.; Zhang, H.; Chen, T.; Yang, C.; Wang, J.; Guo, Z.; Sun, X. Research on the mechanism of plant root protection for soil slope stability. *PLoS ONE* **2023**, *18*, e0293661. [[CrossRef](#)] [[PubMed](#)]
- Löbmann, M.T.; Geitner, C.; Wellstein, C.; Zerbe, S. The influence of herbaceous vegetation on slope stability—A review. *Earth-Sci. Rev.* **2020**, *209*, 103328. [[CrossRef](#)]
- Ding, H.; Xue, L.; Liu, H.; Li, L.; Wang, H.; Zhai, M. Influence of Root Volume, Plant Spacing, and Planting Pattern of Tap-like Tree Root System on Slope Protection Effect. *Forests* **2022**, *13*, 1925. [[CrossRef](#)]
- Li, J.; Wang, X.; Jia, H.; Liu, Y.; Zhao, Y.; Shi, C.; Zhang, F. Effect of herbaceous plant root density on slope stability in a shallow landslide-prone area. *Nat. Hazards* **2022**, *112*, 2337–2360. [[CrossRef](#)]
- Fan, C.C.; Laiy, F. Influence of the spatial layout of vegetation on the stability of slopes. *Plant Soil* **2014**, *377*, 83–95. [[CrossRef](#)]
- Qu, W.; Ji, J.; Chen, L.; Hu, Y. Research on model and test of reinforcing shear strength by vegetation roots in the Loess Plateau of northern China. *J. Beijing For. Univ.* **2017**, *39*, 79–87. [[CrossRef](#)]
- Zhu, J.; Wang, Y.; Wang, Y. An analysis of soil physical enhancement effects of root systems of *Pinus tabuliformis* and *Acer truncatum* based on two models. *Bull. Soil Water Conserv.* **2015**, *35*, 277–282.
- Duan, Q.; Wang, J.; Yang, Y. Improvement of soil shear strength by roots of native herbaceous plants in the dry and hot valley of the Jinsha River and its model prediction. *Bull. Soil Water Conserv.* **2017**, *15*, 87–95.
- Zhang, J. *Research on Comprehensive Benefit Evaluation of Geological Environment Treatment Project in Haizhou Open-Pit Mine*; Liaoning Technical University: Fuxin, China, 2022.
- GB/T 50123-2019; Standard for Soil Test Methods of the Ministry of Housing and Urban Rural Development of the People's Republic of China. China Planning Press: Beijing, China, 2019.

29. Wang, H.; Xue, L.; Ding, H. Analysis of mechanical properties of Elsholtzia root in the small watershed of Reshui River. *Sci. Technol. Eng.* **2022**, *22*, 6894–6903.
30. Hao, G. *Study on the Influence of Herbs in Different Growth Periods on the Stability of Shallow Slopes*; Liaoning Technical University: Fuxin, China, 2022.
31. Liu, Y.; Zhao, Y.; Yang, Y.; Zhang, L.; Liu, W.; Xiong, S.; Duan, Q. Effects of roots of two mixed sowing herbaceous plants on soil shear strength. *Sci. Soil Water Conserv.* **2021**, *19*, 81–88. [[CrossRef](#)]
32. Ouyang, J. *Study on the Mechanical Effect of Vegetation Roots on Soil Consolidation in Ecological Restoration of Abandoned Rare Earth Mines*; Jiangxi University of Science and Technology: Ganzhou, China, 2022.
33. Mahannopkul, K.; Jotisankasa, A. Influences of root concentration and suction on *Chrysopogon zizanioides* reinforcement of soil. *Soils Found.* **2019**, *59*, 500–516. [[CrossRef](#)]
34. Ji, J.; Zhang, C.; Gao, Y.; Kodikara, J. Reliability-based design for geotechnical engineering: Inverse form approach for practice. *Comput. Geotech.* **2019**, *111*, 22–29. [[CrossRef](#)]
35. Ji, J.; Zhang, W.; Zhang, F.; Gao, Y.; Lü, Q. Reliability analysis on permanent displacement of earth slopes using the simplified Bishop method. *Comput. Geotech.* **2020**, *117*, 103286. [[CrossRef](#)]
36. Ji, J.; Wang, C.-W.; Gao, Y.; Zhang, L. Probabilistic investigation of the seismic displacement of earth slopes under stochastic ground motion: A rotational sliding block analysis. *Can. Geotech. J.* **2021**, *58*, 952–968. [[CrossRef](#)]

Disclaimer/Publisher’s Note: The statements, opinions and data contained in all publications are solely those of the individual author(s) and contributor(s) and not of MDPI and/or the editor(s). MDPI and/or the editor(s) disclaim responsibility for any injury to people or property resulting from any ideas, methods, instructions or products referred to in the content.